Journal of Population Therapeutics & Clinical Pharmacology

RESEARCH ARTICLE
DOI: 10.53555/7whn8n07

SYNTHESIS AND CHARACTERIZATION OF MICRO AND MACRO NUTRIENTS FORTIFIED HUMIC SUBSTANCES, PGPB FORTIFIED HUMIC SUBSTANCES, AND ZINC MAGNESIUM FERRITE NANO COMPOSITE FORTIFIED HUMIC SUBSTANCES FERTILIZERS

Tanzila Aslam[1*], Zill-i- Huma Nazli[2], Farhat Jubeen[3], Faiza Nazir[4]

[1*]PhD Scholar, Department of Chemistry, Government College Women University, Faisalabad, Pakistan.
[2]Professor, Department of Chemistry, Government College Women University, Faisalabad, Pakistan.
[3]Assistant Professor, Department of Chemistry, Government College Women University, Faisalabad, Pakistan.
[3]Assistant Professor, Department of Chemistry, Government College Women University, Faisalabad, Pakistan.
[4]Assistant Professor, Department of Chemistry, Government College Women University, Faisalabad, Pakistan.

***Corresponding Author:** Tanzila Aslam
*Email: tanzilaaslam@gcwuf.edu.pk

Received: 27-06-2024 Accepted: 30-07-2024 Published: 28-08-2024

ABSTRACT

All of Pakistan's provinces contain coal resources of 185 billion tones. Most of the Pakistani coal is utilized to produce energy, which is not environmentally beneficial. As a result, it is imperative to discover novel approaches to enhance the environmentally beneficial use of coal, and that's why scientists are so interested in it. This paper compares the synthesis of bio, organic, and nano fertilizers. It was done to find out how well native coal samples could be used for alkaline extraction of humic substances (HS) like fulvic acid (FA) and humic acid (HA). The isolation of PGPB, and green synthesis of MgZn ferrite nano-composite were also done, which have a pH-buffering alkalinity, a cation exchange capacity, positive biological functions, and is widely used in agriculture. Using 0.1 M KOH, the coal samples collected from Punjab and Baluchistan, Pakistan, were examined for HS extraction. After shaking for 6-hour interval, the maximum percentage yields were obtained of FA and HA (71.5% and 37.5%, respectively) in coal sample number 5 whereas minimum yields of FA and HA were obtained 46 % and 21.5 % respectively, in coal sample no. 3. The highest values of the E4/E6 and E3/E5 ratios, which were computed using UV-visible spectroscopy to assess the degree of humification of HS samples, are 1.99 for HA and 222.52 for FA of sample no. 7. The PGPB isolates PSBW-R, KSBW-R, and AZOW-R produced both gram-positive and gram-negative findings. All isolates were able to metabolize all kinds of carbohydrates and shown a positive growth response when the pH was changed from 8 to 10 as well as at 40 and 50 ˚C temperatures. Coal, HA, FA, macro and micronutrients fortified HS, PGPB fortified HS, and MgZn ferrite nano-composite fortified HS

were all characterized using Fourier transform infrared spectroscopy, and HPLC. The green synthesized nanocomposite was characterized using XRD, DLS, SEM, and TEM. It has been demonstrated that all fertilizers contain carboxylic acid, amino, and hydroxyl functional groups, aliphatic and aromatic hydrocarbons, and intermolecular hydrogen bonds. Statistix 8.1 software was used to examine the design's experimental findings. In which the LSD all-pairwise comparisons test means of FA and HA are not significantly different from one another as the P-value is less than 0.05.

Keywords: Humic substances, Humic acid, Fulvic acid, nano-composite, PGPB, Phosphate and Potassium solubilizing bacteria, nitrogen-fixing bacteria

1. INTRODUCTION

Lignite is an energy source and a big source of humic substances, accounting for 45% of reserves of low-rank coal globally. Coal-derived humic substances are big polymers of organic compounds that nourish soil microbes, enhancing their activity and diversity (Zykova, et al., 2024). Organic macromolecules with complicated structures include carbonyl, phenolic, hydroxyl, carboxylic, amine, amide, and aliphatic moieties are known as humic substances. Because of their unique chemical characteristics, humic substances can be used in agriculture, biomedicine, industry, and surroundings (Jarukas, et al., 2021).

They increase microbial presence and help create a balanced ecosystem that positively impacts plant health (Turan, et al., 2022). Humic substances modify the soil environment, making it less hospitable to soil-borne diseases. The growth of beneficial microbes can suppress pathogens, consequently improving plant resilience. By boosting nutrient efficiency, humic substances reduce the dependency on synthetic fertilizers (Li, et al., 2022).

The soil has become deficient in both macro and micronutrients as a result of intensive agricultural practices. This has led to decrease in soil fertility and productivity rate (Dhayal et al., 2023). Continuously and inappropriate application of chemical fertilizers can significantly affect the soil pH, which has adverse impacts on the bacterial diversity and physicochemical properties of soil (Al-Saif et al., 2023). Because of their high pH, calcareous soils have limited macro and micronutrients availability. The excessive consumption of chemical fertilizers in recent decades has created multiple environmental problems all over the world (Rasouli et al., 2022).

According to Dhayal et al. (2023), humic substances (HS) are essential for plant nutrition and soil fertility. HS are applied in fields to make the soil fertile with balanced quantity of nutrients, altering hazardous compounds by breaking them down and ultimately preparing the essential media for soil organisms to survive (Turan et al., 2022). Application of HS enhances plant height, spike density/m^2, grain yield, grain weight, protein content and gluten content. HS are used to control the amount of stress hormones that plants release in response to both abiotic and biotic stresses (Tahoun et al., 2022).

Three types of microbes are present in the environment including symbiotic, associative and pathogenic which can affect plant physiology such as growth rate, nutrition level and defense mechanisms. Bacteria gain nitrogen and carbon metabolites from plant roots (rhizosphere) or inside the root (endosphere) and inhabit aerial parts (phyllosphere) of the plants which move through xylem vessels in the whole plant. The most common plant growth promoting bacteria (PGPB) belong to the genera Pseudomonas, Enterobacter, Bacillus, Acinetobacter, Arthrobacter, Burkholderia and Paenibacillus. These bacteria are known to enhance plant immunity against pathogens and provide phytohormones, soluble phosphate, zinc, potassium, and nitrogen (Balasjin et al., 2022).

The rapidly increasing rate of global population, which is assumed to exceed 9.4 billion in 2050 is one of the foremost and major factors causatives to the dire need for the advancement of efficient and effective agricultural tools to alleviate poverty and global hunger (Ndaba et al., 2022).

Nanoparticles can carry foreign substances into plant cells due to their small size, while protecting foreign substances from degradation. Nanoparticles can enter the plant system through several pathways such as through diffusion, root hairs, stomata, and cracks on the surface of the leaf (Wang et al., 2023). The main aim of this study was to form such types of fertilizers that are ecofriendly, non-

toxic, more effective, make the soils soften and fertile, and improve yield in comparison to other fertilizers.

2. MATERIAL AND METHOD

2.1 Collection of samples

The agricultural waste, coal, and soil samples were collected from different areas of Punjab, and Baluchistan, Pakistan as shown in (Table 1). The waste was crushed into granules roughly below 40.0 mm in diameter (Salama et al., 2022; Fincheira et al., 2023).

Table: 1 Quantity of collected samples used for lab and field experiments

Sr. No.	Collected Samples	Types	Qty for Lab experiment	Qty for Field experiment
2	**Coal**	Khushab	10 g	0 Kg
		Dandot	10 g	0 Kg
		Khewra	10 g	0 Kg
		Thar	10 g	10 Kg
		Deraa Bugti Kan No. 2	10 g	0 Kg
		Deraa Bugti Kan No. 3	10 g	0 Kg
		Deraa Bugti Kan No. 4	10 g	0 Kg
		Deraa Bugti Kan No. 5	10 g	10 Kg
3	**Soil**	Wheat grown rhizosphere soil (Malokay, Narowal)	1 g	10g
		Paddy rice grown soil (Shaheed Mehfoz Garrison Cantt, Lahore)	1 g	10g

2.2. Manufacturing of fertilizers

Different fertilizers were synthesized to enhance soil fertility, crop health, and productivity.

2.2.1 Micro and macronutrients fortified humic substances (HS)

2.2.1. (a) Extraction of humic substances from coal

All coal samples were weighed (10 g) and added into 1000 ml of 0.5M of KOH solution. The alkaline extraction was carried out by orbital shake flask procedure for 8 hours at 150 rpm at 35 ^{0}C temperature After that all mixtures were centrifuged using falcon tubes and maintained pH at 1.6 to 2 with conc. 0.5M HCl (about 30 ml to 50 ml acid consumed). After maintaining pH, both mixtures were kept overnight at room temperature. Standing mixtures were filtered and the filtrate of the standing mixture contained fulvic acid while precipitates of solid particles contained humic acid. Evaporate the maximum water from fulvic acid samples at 60 ^{0}C temperature for 3 to 4 hours to get pure fulvic acid (Malyushevskaya et al., 2023).

2.2.1. (b) Micro and macronutrients fortified humic substances (HS)

Micro and macronutrients fortified humic substances (HS) complexed fertilizer was prepared by using this method (Ichwan et al., 2022).

2.2.2 PGPB-fortified humic substances (HS)

2.2.2. (a) Isolation of plant growth promoting bacteria from soil

Isolation of bacteria was done according i.e., potassium-solubilizing bacteria (Fatharani and Rahayu, 2018), nitrogen-fixing Azotobacter (Din et al., 2019), Phosphate solubilizing bacteria (Panhwar et al., 2012; Awais et al., 2019).

2.2.2. (b) PGPB-fortified humic substances

PGPB and humic substances are auspicious choices in agriculture for reducing the usage of mineral and pesticide fertilizers. PGPB-fortified humic substance fertilizer was prepared by using this method (Olivares et al., 2015; da Silva et al., 2021).

2.2.3 Magnesium Zinc Ferrite ($MgZnFe_2O_4$) nanocomposite fortified humic substances

2.2.3. (a) Green Synthesis of Magnesium Zinc Ferrite ($MgZnFe_2O_4$) Nanocomposite

Following the method outlined by Taha et al. (2018), the experimental procedure was modified by replacing Ni (Nickel) with Mg (Magnesium) as the metal component. Instead of bovine gelatin, moringa leaves extract was utilized as a natural stabilizing or reducing agent (Taha et al., 2018).

{[$(Mg(NO_3)_2$ + $Zn(NO_3)_2$ + $Fe(NO_3)_3$ + H_2O] + Moringa leaves extract} → Stir and heat
↓ **For Reaction Process**
add KOH to adjust pH =11 → [Stir + heat] for 5h allow ppts to age → ppt formed after 5h
↓**For the Drying and Calcination Process**
placed in microwave for 120 min at 120 °C for drying → Dried ppt washed at pH 7.00

2.2.3. (b) Magnesium Zinc Ferrite ($MgZnFe_2O_4$) nanocomposite fortified HS

The co-precipitation method was used to chelate nanocomposite with humic acid. The 300 mg/L of HS solution was prepared and then added 2.043 g of prepared nanocomposite into 50 mL HS solution and stirred for 48 h at 25 °C. Then precipitates were obtained by centrifuging the solution for 08 min at 600 rpm (Sable et al., 2022; Al-Hayani and Sallume, 2023).

2.4 Characterization:

2.4.1 Proximate analysis of collected samples

The volatile matter, ash, moisture, and carbon content in the collected coal, soil, and wheat samples were determined by ASTM (American Society for Testing and Materials) method (Salama et al., 2022; Ennan et al., 2022).

2.4.2 Biochemical, Physiological, and Gram staining characteristics of Bacteria

Biochemical, physiological, and gram-staining characteristics of Potassium solubilizing bacteria (Fatharani and Rahayu, 2018), Phosphate solubilizing bacteria (Panhwar rt al., 2012; Mohite, 2013; Awais et al., 2019), and Nitrogen-fixing bacteria (Din et al., 2019) were performed.

2.4.3 Instrumental characterization of samples

UV-Vis, FTIR, HPLC, SEM, TEM and XRD, DLS techniques were used to characterize the samples (Taha et al., 2018; Tatarchuk et al., 2020; Sharif et al., 2022).

2.5 Statistical Analysis

The data was analyzed using analytical techniques and tables were made in the form of LSD All-Pairwise Comparisons Test mean yields of FA and HA extracted from coal samples, which were found to be statistically best. By using the software Statistix 8.1 all data was subjected to statistical analysis (Steel et al., 1997).

3. Results and Discussion

3.1 Isolation of bacteria and their biochemical, physiological, and gram-staining characteristics of Bacteria

The bacterial isolates were recognized as phosphate-solubilizing which can solubilize $Ca_3(PO_4)$, potassium-solubilizing which can solubilize potassium, and nitrogen-fixing bacteria which can produce ammonia. There were 06 rhizobacterial strains isolated and purified from wheat and paddy rice rhizosphere soils (Fig. 1). The isolates were designated as PSBW, PSBR, KSBW, KSBR, AZOW, and AZOR and characterized as shown in (Table 2).

Calcium solubilization reaction of PGPB:

$$Ca_3(PO_4)_{2\,(s)} + 2H^+ \rightarrow 3Ca^{2+} + 2HPO_4^{2-}$$

Potassium solubilization reaction of PGPB:

$$KAlSi_3O_{8\,(s)} + H^+ \rightarrow K^+ + HAlSi_3O_8$$

Nitrogen fixation reaction of PGPB:

$$N_{2(g)} + 8H^+ + 8e^- + 16ATP + \textit{Nitrogenase bacterial enzyme} \rightarrow 2NH_{3(g)} + H_{2(g)} + 16ADP + 16Pi$$

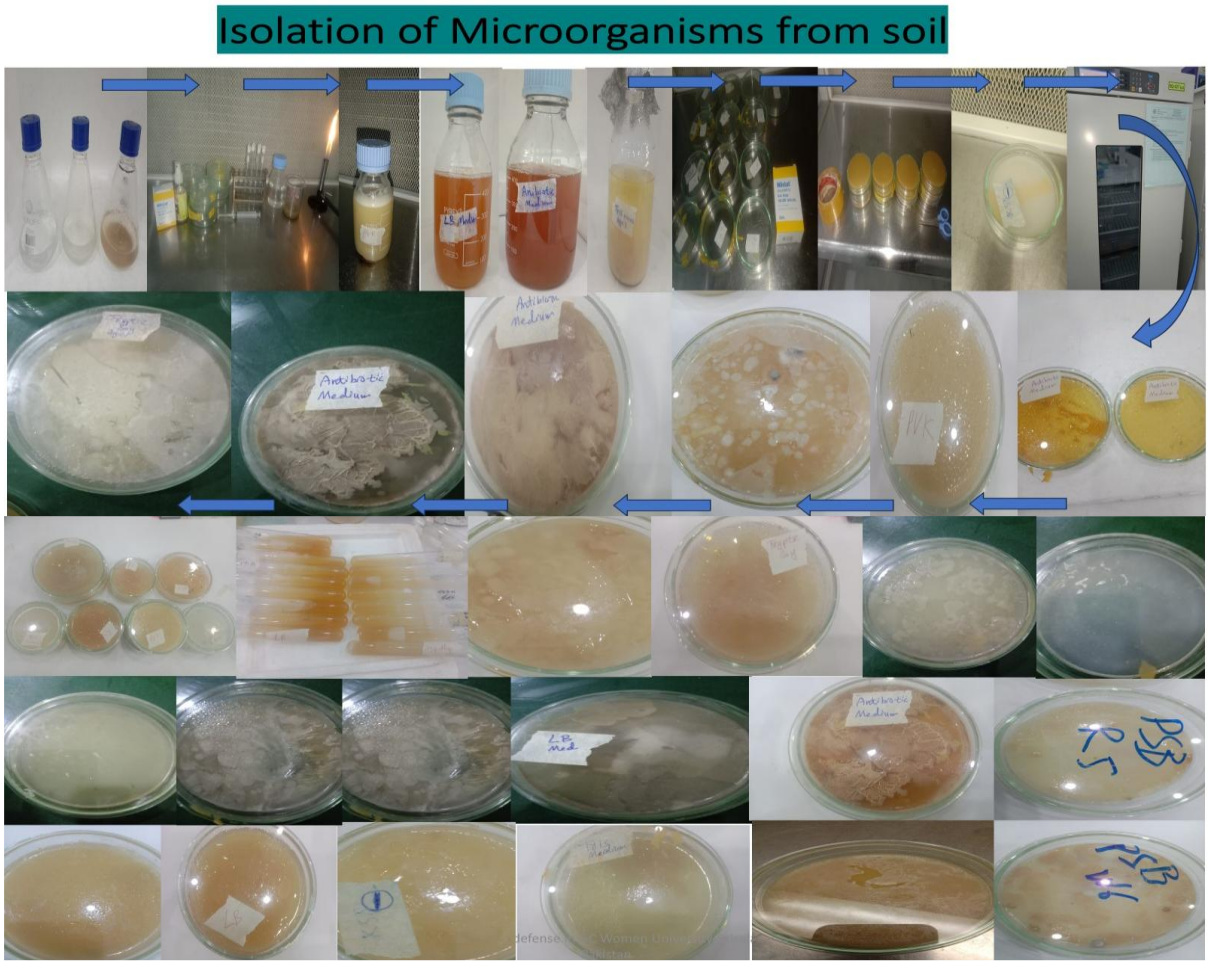

Fig. 1 Isolation of phosphate-solubilizing, potassium-solubilizing and nitrogen-fixing bacteria from soil

Table 2: Biochemical, Physiological, and Gram staining characteristics of Potassium/ Phosphate Solubilizing Bacteria and Nitrogen-fixing Bacteria

Biochemical, Physiological, and Gram staining Tests	Bacterial Isolates					
	(PVK media)		(KSB media)		(Azo media)	
	PVK W	PVK R	KSB W	KSB R	AZO W	AZO R
Citrate utilization	+	+	–	–	+	+
Indole production	–	–	–	–	–	–
Vogus Proskauer Test	–	–	–	–	+	+
Methyl red Test	–	–	+	+	+	+
Oxalic acid	+	+	+	+	–	–
Glucose	+	+	+	+	+	+
Mannitol	+	+	+	+	+	+
Fructose	+	+	+	+	+	+
Sucrose	+	+	+	+	+	+
Xylose	–	–	+	+	–	–
Motility	+	+	+	+	+	+
Catalase	+	+	+	+	–	–
Urease	+	+	–	–	+	+
Amylase	+	+	+	+	+	+
Protease	+	+	+	+	+	+
Pectinase	+	+	+	+	–	–
H_2S production	–	–	+	+	+	+
Nitrate reduction	+	+	+	+	+	+
Triple Sugar Iron	+	+	+	+	+	+
Urease	+	+	+	+	+	+
Lactose	–	–	+	+	–	–
Oxidase	+	+	+	+	+	+
Gram Straining (Positive/ Negative)	+ (Bacillus)	– (Bacillus)	+ (Bacillus)	– (Bacillus)	– (Rhizobium)	– (Rhizobium)
Shape	Rod-shaped	Rod-shaped	Irregular shaped	Undulate shaped	circular	circular
Smell	pungent smell	rotten egg-like smell	musty smell	Earthy smell	No smell	No smell
Surface	Mucoid	Shiny	luminous	Shiny	Opaque	Transparent
Margin	Wavy	Smooth	smooth	smooth	curled	mucoid
Colony counting	4mm	3mm	3mm	3mm	2mm	3mm
Color	Off white	Greenish white	Yellowish brown	Greenish	pale white	Yellowish white

				Yellow		
Solubilization Index after 4 days of incubation	3.68	2.57	2.2	2.0	2.4	2.3
Solubilization Index after 8 days of incubation	4.7	4.3	3.5	3.3	3.2	3.0
Effect of pH on growth (pH = 8)	+	+	+	+	+	+
Effect of pH on growth (pH = 10)	+	+	+	+	+	+
Effect of Temperature on growth at 40 ˚C	+	+	+	+	+	+
Effect of Temperature on growth at 50 ˚C	+	+	+	+	+	+

3.2 Proximate analysis of collected samples

The results of the proximate analysis of seven coal samples are given in Table 3. The moisture content is found highest in sample No.4 at 61.5% and lowest in sample No.5 at 48.27% respectively. The Ash content of coal samples is found 20.4% in sample No.5 the highest and 3.16% in sample No.1 the lowest. In the absence of moisture and ash contents, the Volatile content of coal samples is found 6.65% for sample No.1 as the highest on the other hand 3.98% is found for sample No.4 as lowest (Donahue and Rais, 2009)

Table 3 Proximate analysis of coal

Sample#	Volatile content%	Moisture Content%	Ash Content%
1. (Deraa Bugti Kan No.5)	6.65± 0.14	31.30±0.63	3.16±0.5
2. (Khushab)	5.83±0.6	58.60±0.5	5.08±0.4
3. (Dandot)	6.5±1.20	50.50±0.7	5.4±0.64
4. (**Deraa Bugti Kan No.4)**	3.98±0.98	61.50±0.9	4.1±0.71
5. (**Deraa Bugti Kan No.3)**	5.66±2.12	48.27±0.65	20.4±0.91
6. (**Deraa Bugti Kan No.2)**	5.06±0.63	51.10±0.55	14.24±0.61
7. (Khewra)	6.6±0.70	60.70±0.8	24.4±0.59

3.3 Statistical analysis of extraction yield of humic substances

Analysis of variance CRD ANOVA was applied to collected HA and FA yields data and results were shown in Table 4 where alpha is 0.05, critical T Value is 2.365 and the P-value < 0.05 shows significant effects on extraction yield of both fulvic acid and humic acid while no interaction exists between these factors as the P-value is less than 0.05.

Table 4 LSD All-Pairwise Comparisons Test of FA and HA

Samples	LSD All-Pairwise Comparisons Test of FA by Sample	LSD All-Pairwise Comparisons Test of HA by Sample
1. (Deraa Bugti Kan No.4)	59.000d	26.500d
2. (Dandot)	62.500c	28.500c
3. (**Deraa Bugti Kan No.2)**	46.000f	21.500e
4. **(Khushab)**	66.000b	33.500b
5. (**Deraa Bugti Kan No.5)**	71.500a	37.500a
6. (**Deraa Bugti Kan No.3)**	56.000e	26.500d
7. (Khewra)	54.000e	26.000d
Statistical results (The trend of both sample's % yield is found as (Deraa	There are 6 groups (a, b, etc.) in which the means are not	There are 5 groups (a, b, etc.) in which the means are not

Bugti Kan No. 5) > (Khushab) > (Dandot) > (Deraa Bugti Kan No. 4) > (Deraa Bugti Kan No. 3) > (Deraa Bugti Kan No. 2) > (Khewra).)	significantly different from one another.	significantly different from one another.

3.4 Instrumental characterization of samples

3.4.1 Ultraviolet-visible (UV-VIS) spectroscopy of humic substances

Isolated humic substances (humic and fulvic acids) from coal using KOH as an extractant were characterized by recording absorbance on a UV-VIS spectrophotometer as shown in Table 5 (a) and (b). The absorbance was observed at 350nm, 465nm,550nm, and 665nm. The humification index is the ratio of coefficients of E_3/E_5 and E_4/E_6. Humic substances formed at the initial humification stage indicated by absorbance at 365nm and absorbance at 665nm indicate the humic substances formed in well-humified organic matter. ΔlogK coefficient was used to characterized humification degree.

ΔlogK of HA = (log (Abs465) – log (Abs665))

ΔlogK of FA = (log (Abs365) – log (Abs565))

Table 5 (a) and (b) UV-VIS spectral properties of HA and FA

(a)UV-VIS spectral properties of HA

Sample#	E4/E6 Ratio	Log K
1	1.735	0.239
2	0.822	0.085
3	1.09	0.037
4	1.079	0.033
5	1.564	0.194
6	1.364	0.134
7	1.994	0.299

(b) UV-VIS spectral properties of FA

Sample#	E3/E5 Ratio	Log K
1	23.429	1.06
2	21.629	1.026
3	38.179	1.275
4	71.705	1.328
5	26.956	1.087
6	132.936	1.173
7	222.524	1.195

Both fulvic acid and humic acid showed extensive absorption in the UV range (200–400 nm) because of the different chromophores they contained, including conjugated double bonds and aromatic rings. UV range (200–300 nm), which is associated with conjugated systems, aliphatic moieties, carboxylic acids, phenolic groups along with aromatic structures. As the wavelength increased, the absorbance of the HA spectrum gradually decreased, which showed a more complex and aromatic structure (Fig. 2(b)). However, as shown in Fig. 2(a), the FA spectrum decreases more sharply, indicating a simpler and less aromatic complex composition.

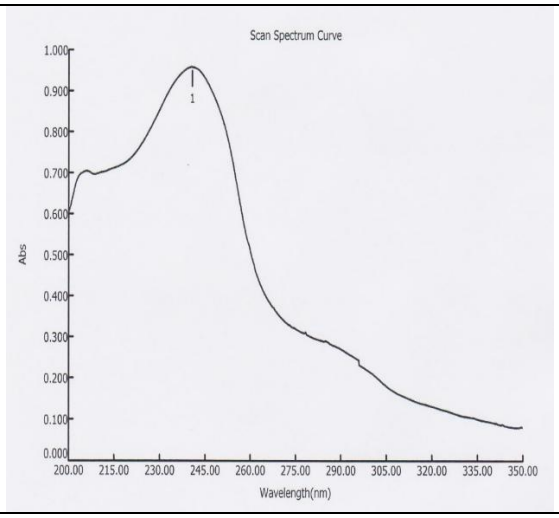

Fig. 2 (a) UV spectrum of FA

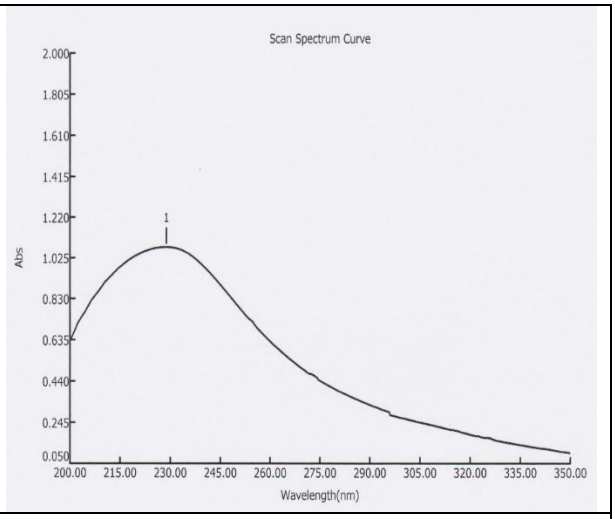

Fig. 2 (b) UV spectrum of HA

3.4.2 Dynamic Light Scattering (DLS) Analysis of MgZn Ferrite nanocomposite

Zeta sizer is an instrument of nano range which measures the three fundamental characteristics of particles or molecules in liquid medium. These three characteristics are particle size, zeta potential and molecular weight. By using zeta sizer particle size, zeta potential and molecular weight can be measured over wide range of concentrations. Zeta sizer analysis of MgZn Ferrite nanocomposite is performed using Malvern zeta sizer (Malvern ZS). Particle size distribution of MgZn Ferrite nanocomposite is shown in **Fig. 3**. Zeta analysis of MgZn Ferrite nanocomposite reveals that Z-Average size of nanocomposite in (d.nm) is 1197 and the polydispersity index (PdI) is 0.381 (Chauhan *et al*., 2012 and Jaeger *et al*., 1991)..

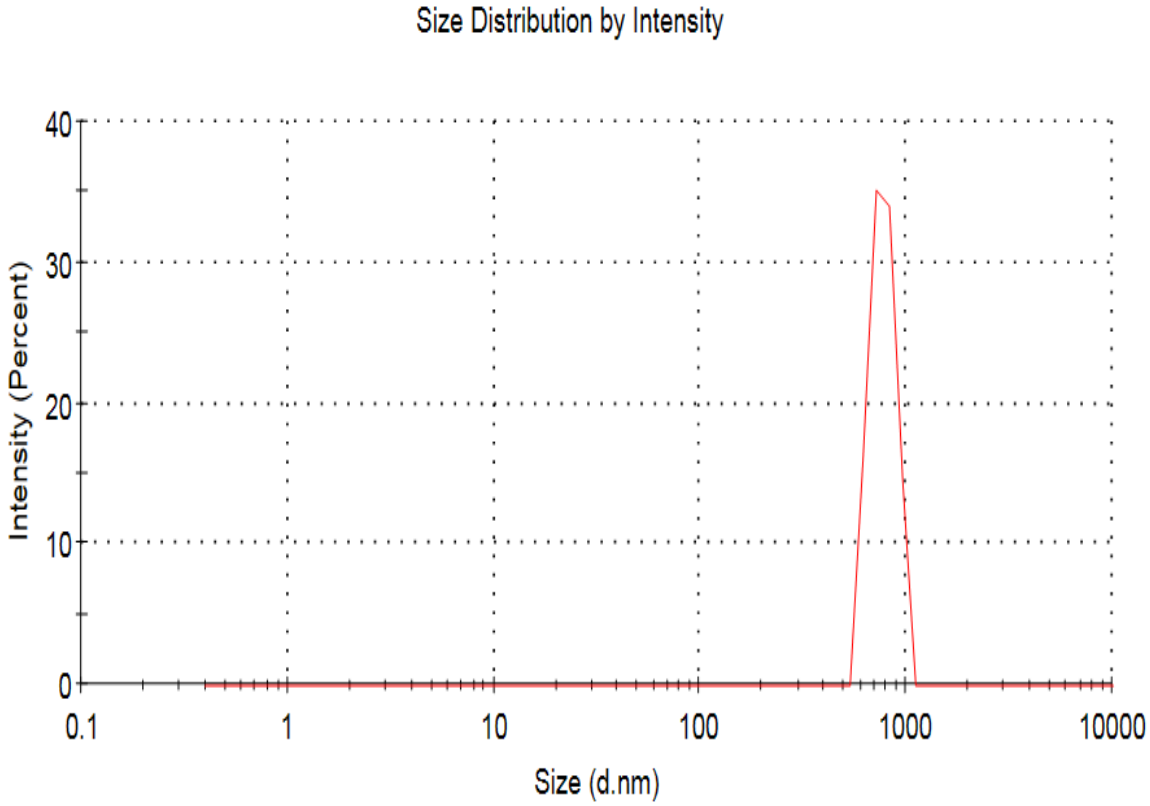

Fig. 3. Size distribution by intensity of MgZn Ferrite nanocomposite

3.4.3 Fourier Transform Infrared (FTIR) Spectroscopy

FTIR analysis of HS:

Infrared spectrum is important to determine the structural information about the molecules. The FTIR spectra contained the following groups within the range: OH phenolic 3666 cm^{-1}, OH in hydrogen boning form at 3300-3700 cm^{-1}, NH at 3550 cm^{-1} , CH aliphatic at 2892 cm^{-1} and 2823 cm^{-1} , carbon, carbon triple bond at 2137 cm^{-1} , C=C in conjugated form at 1633 cm^{-1} , C-O at 1019 cm^{-1} , C-Cl at 751 cm^{-1} .

Spectra of coal, HA and FA are shown in **Fig. 4 (a).** In all these spectra the broad band at 3430 cm^{-1} represents OH group and absorption band at 2900-3300 cm^{-1} showed the presence of CH and CH_2 groups. The C=O group of a carboxylic acid is responsible for the absorbance band at 1700 cm^{-1}. C=C group is represented by a strong band between 1500 cm^{-1} and 1650 cm^{-1}. A few peaks between 1100 cm^{-1} and 1200 cm^{-1} represent the stretching of the Si-O and C-O atoms. Peaks between 450 cm^{-1} and 600 cm^{-1} indicated the existence of the C-Cl group since HCl is used to treat coal in order to maintain pH. The -SO3 and -CN stretching vibrations can be attributed to the bands centered on 1234 cm^{-1} and 1080 cm^{-1}, respectively **(**Saikia et al., 2007; Eshwar et al., 2017; Hansima et al., 2022)

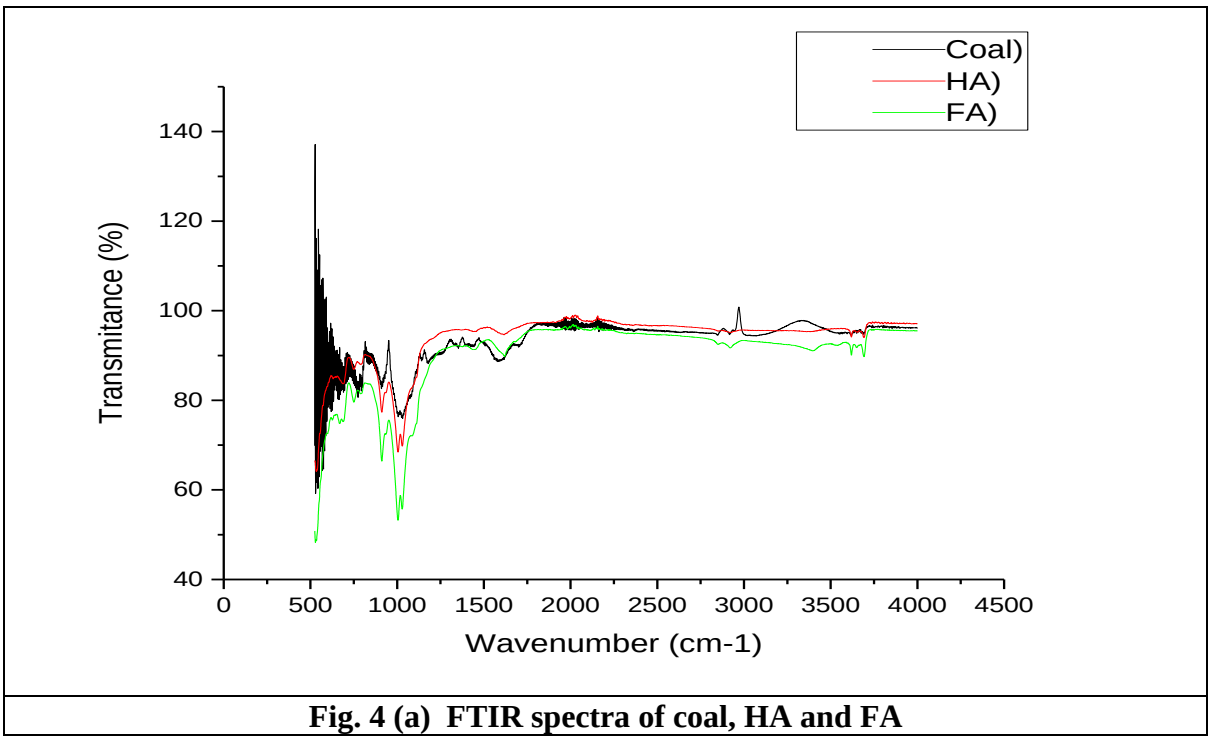

Fig. 4 (a) FTIR spectra of coal, HA and FA

FTIR analysis of MgZn Ferrite nanocomposite:

FTIR analysis of MgZn Ferrite nanocomposite was performed using Bruker spectrometer in the wave number range from 4000cm^{-1} to 500cm^{-1}. FTIR spectra of MgZn Ferrite nanocomposite is shown in **Fig 4 (b).** The FTIR absorption bands are obtained at 3750.42cm^{-1}, 3649.34 cm^{-1}, 3357.34 cm^{-1}, 1541.63 cm^{-1}, 1339.08 cm^{-1} and 540.50 cm^{-1}. The absorption band at 3750.42 cm^{-1} is due to stretching vibrations of C=C bonds. This band is accordance with Sharif *et al*., (2022) due to stretching vibrations of C=C bonds. A major peak was identified at 3649.34 cm^{-1} due to the O–H stretching vibrations of polyphenolic groups. This peak is related to Venkateswarlu *et al*., (2014) who observed O–H stretching vibrations of polyphenolic groups. In addition, absorption band at 3357.34 cm^{-1} is due to O–H stretching vibrations (Tatarchuk et al., 2020). The broad peak at 1541.63 cm^{-1} due to the CN stretching vibrations modes of amido bond (Sharif et al., 2022). The absorption peak at 1339.08 cm^{-1} is due to C–N stretching of aromatic amines. This FTIR spectra confirms the synthesis of MgZn Ferrite nanocomposite and the presence of polyphenolic groups in green synthesised MgZn Ferrite nanocomposite (Taha et al., 2018; Sharif et al., 2022).

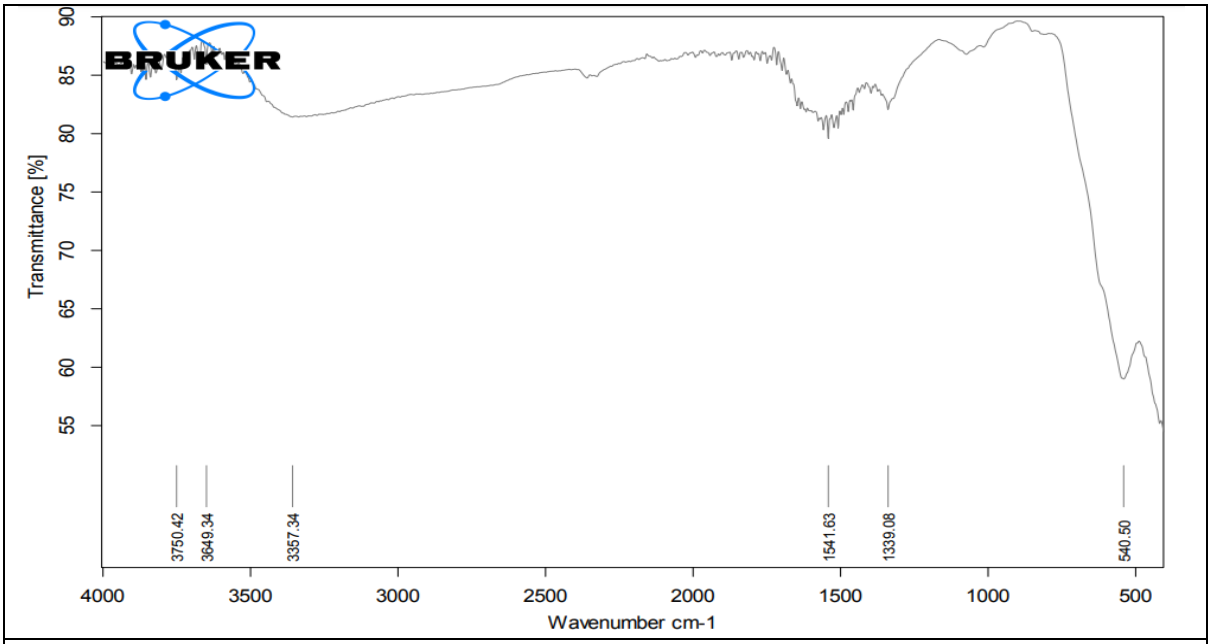

Fig. 4 (b) FT-IR spectra of MgZn Ferrite nanocomposite

3.4.4 X-Ray Diffraction (XRD) analysis

3.4.4 (a) X-Ray Diffraction (XRD) analysis of Coal, HA, and HA

Coal, FA, and HA XRD spectra are displayed in **Fig. 5(a).** The extracted fulvic acid and humic acid were amorphous and present in small amounts, as evidenced by the serrated and disordered fulvic acid and humic acid spectra when compared to the coal's XRD spectra. Coal's amorphous and crystalline carbons are found in the γ (21◦) and G (25◦) bands, respectively. Additionally, the molecular configurations of fulvic acid and humic acid are disordered and contain both aliphatic and aromatic carbons. Consequently, these variables may have a significant impact on chemical characterization. Anhydride, carboxyl groups, hydroxyl groups, and other oxygen-containing functional groups are the primary constituents of the functional groups of coal, fulvic, and humic acids (Saikia et al., 2007; Nazarbek et al., 2022; Wu et al., 2023).

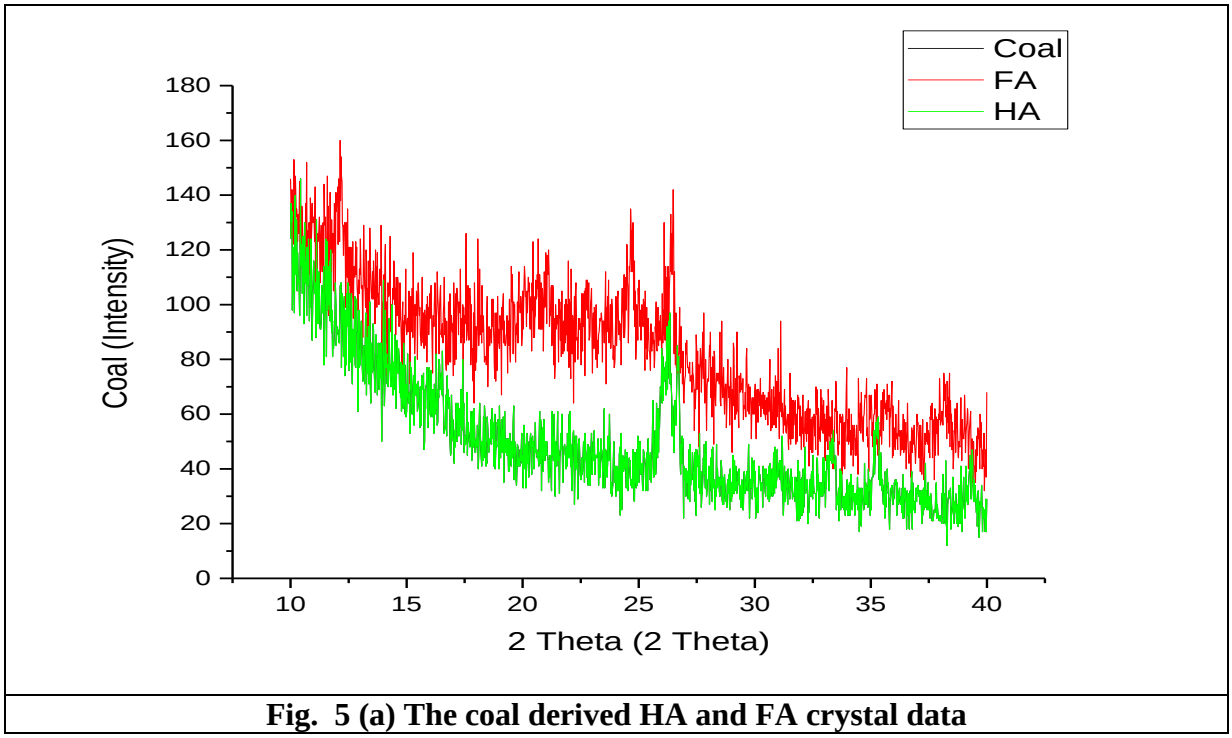

Fig. 5 (a) The coal derived HA and FA crystal data

3.4.4 (b) X-Ray Diffraction (XRD) analysis of MgZn-ferrite nanocomposite

XRD pattern of the freshly prepared MgZn-ferrite nanocomposite is shown in **Fig. 5 (b)**. The XRD peaks are observed at 30.40°, 30.80°, 32.50°, 34.60°, 37.00°, 43.70°, 48.50° and 56.80° 2θ values and these 2θ values have respective miller indices (513), (060), (602), (444), (604), (606), (646) and (757). The nanocomposite displays the sharp peaks in the XRD pattern which clearly show that the product is purely crystalline in structure consists of cubic unit cell and verified that the product is very pure. For the impurities, there should be an extra peak in the XRD pattern. The broadening of the peaks also clearly represents that the product is in the nanometer range and the size of most of the particles is under 100nm (Taha et al., 2018; Tatarchuk et al., 2020; Sharif et al., 2022).

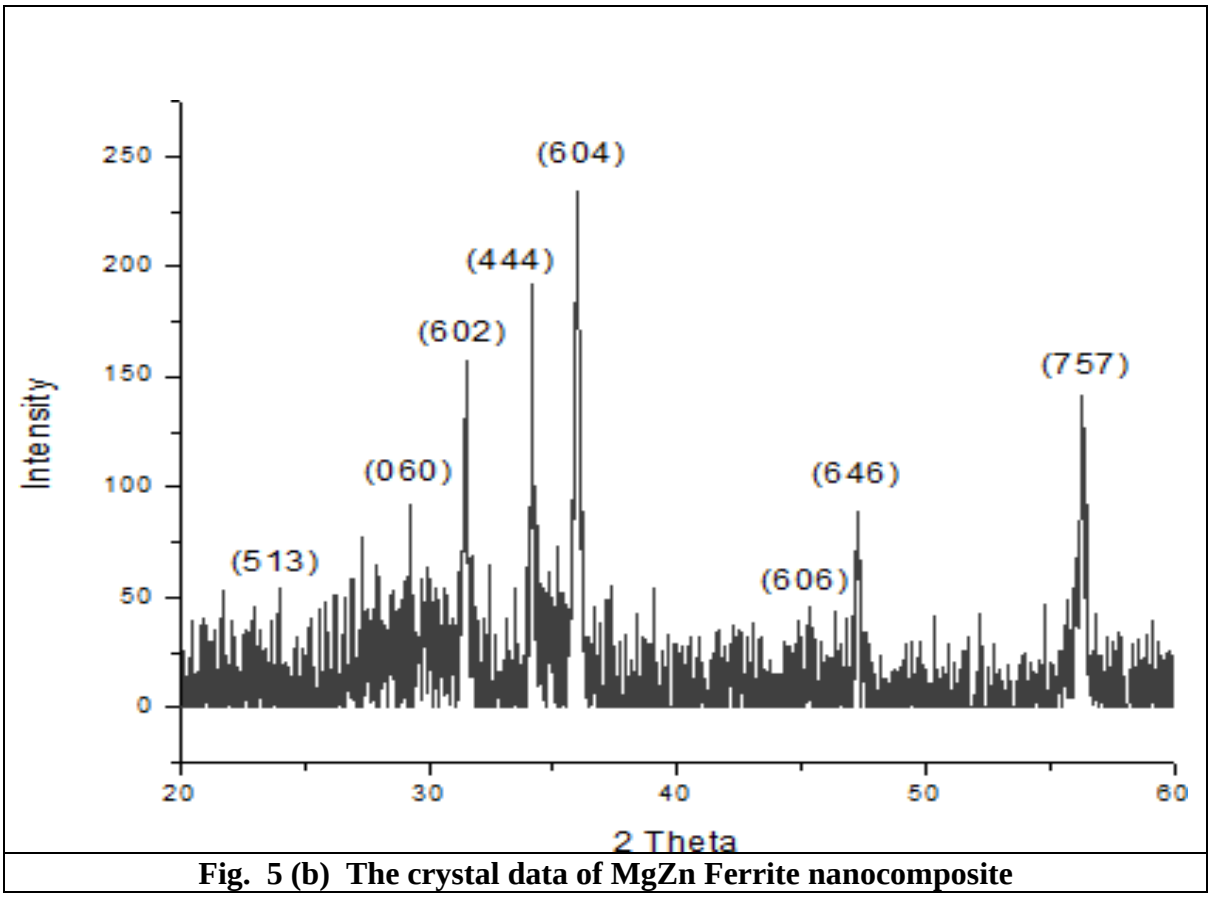

Fig. 5 (b) The crystal data of MgZn Ferrite nanocomposite

3.4.5 Scanning electron microscopy (SEM) of MgZn Ferrite nanocomposite

The Scanning electron microscopy (SEM) results tell us about the size, morphology, shape, and porosity of the nanoparticles. The SEM images of the MgZn Ferrite nanocomposite at various magnifications are illustrated in Fig. 6 (a, b, c). The SEM results of Fig. (a) and (b) show that the nanocomposite has merged surfaces and are mostly irregular in shape and the size of nanocomposite lies in the 50um range. Fig. (c) shows that the size of nanocomposite is in the range of 100nm. At high magnification in Fiig. (c) the rough edges of the nanocomposite are visible (Taha et al., 2018; Tatarchuk et al., 2020; Sharif et al., 2022).

Fig. 6 (a) SEM images of green synthesized MgZn Ferrite nanocomposite	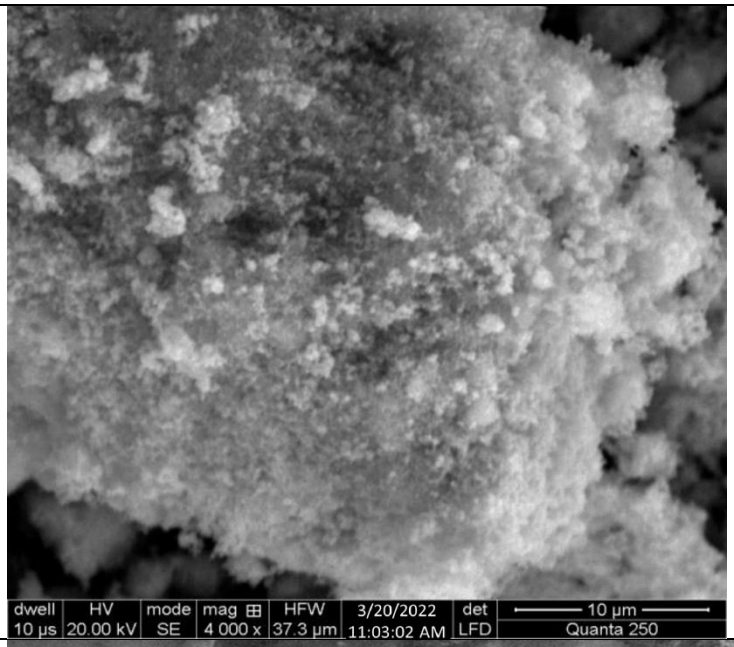
Fig. 6 (b) SEM images of green synthesized MgZn Ferrite nanocomposite	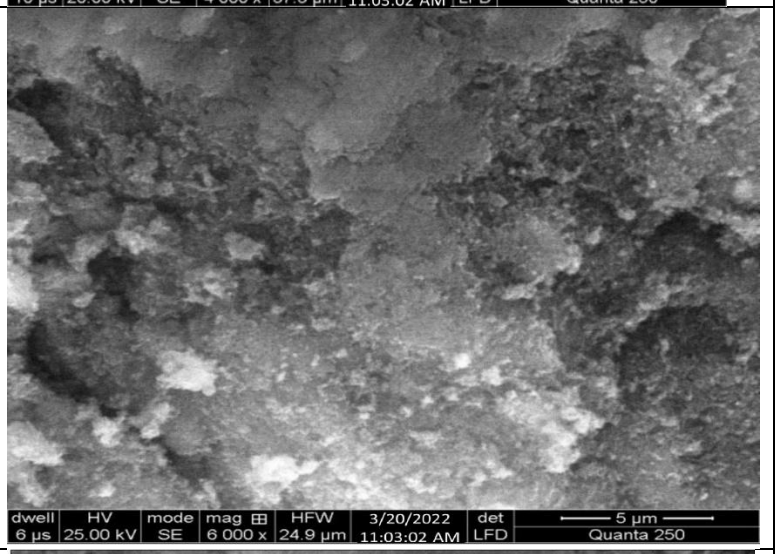
Fig. 6 (c) SEM images of green synthesized MgZn Ferrite nanocomposite	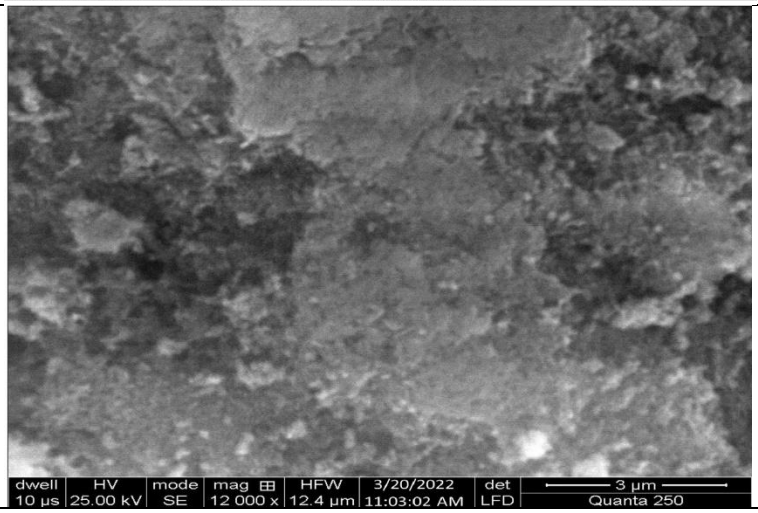

3.4.6 Transmission electron microscopy (TEM) observations

Transmission electron microscopy (TEM) provides us with useful information relating to the shape, atomic size, and chemical structure of the nanoparticles. TEM images of the MgZn Ferrite nanocomposite at several magnifications is shown that the size size of most of the nanocomposite is

more than 100nm and most of the nanocomposite are irregular in shape as shown in **Fig. 7** (Taha et al., 2018; Tatarchuk et al., 2020; Sharif et al., 2022).

Fig. 7 TEM images of green synthesized MgZn Ferrite nanocomposite

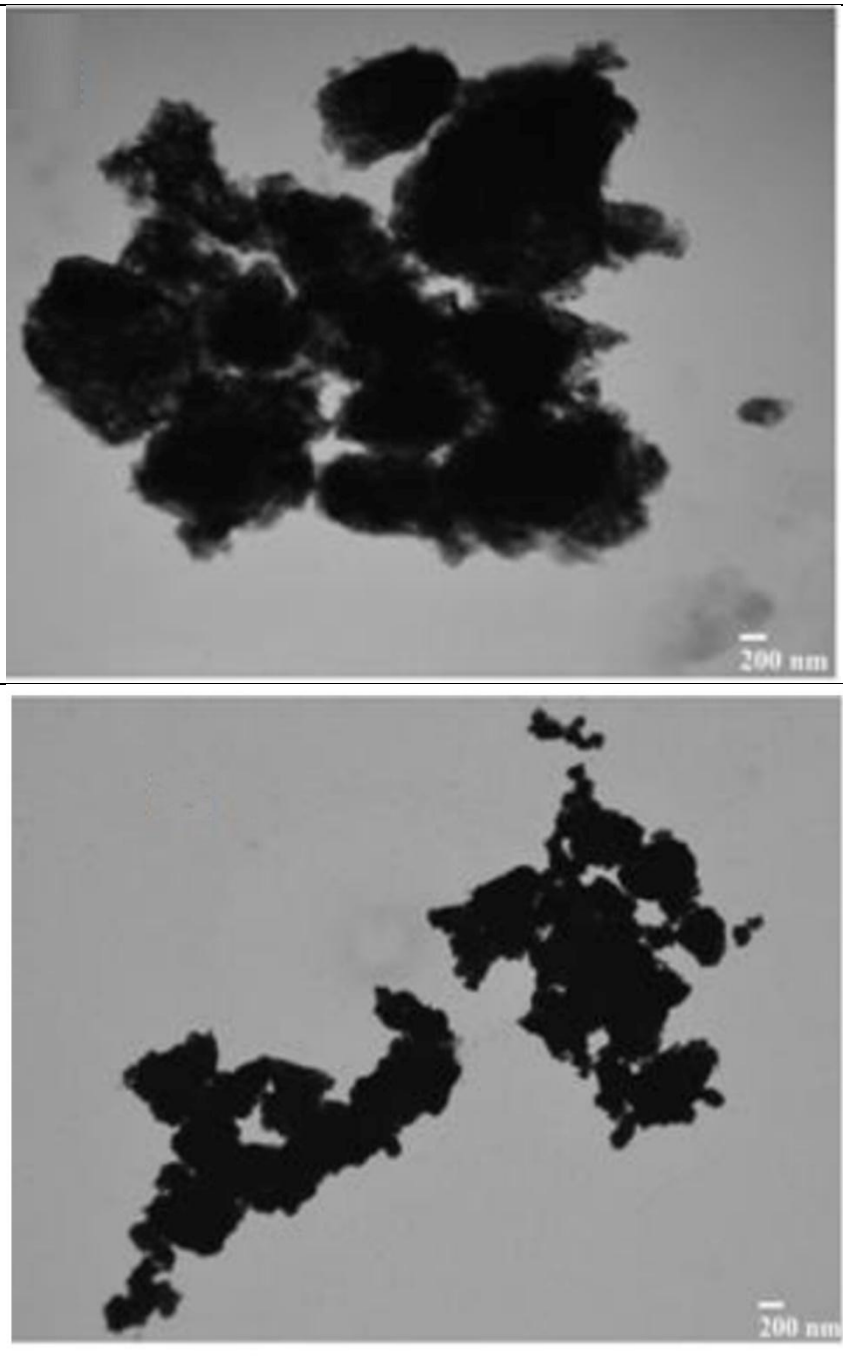

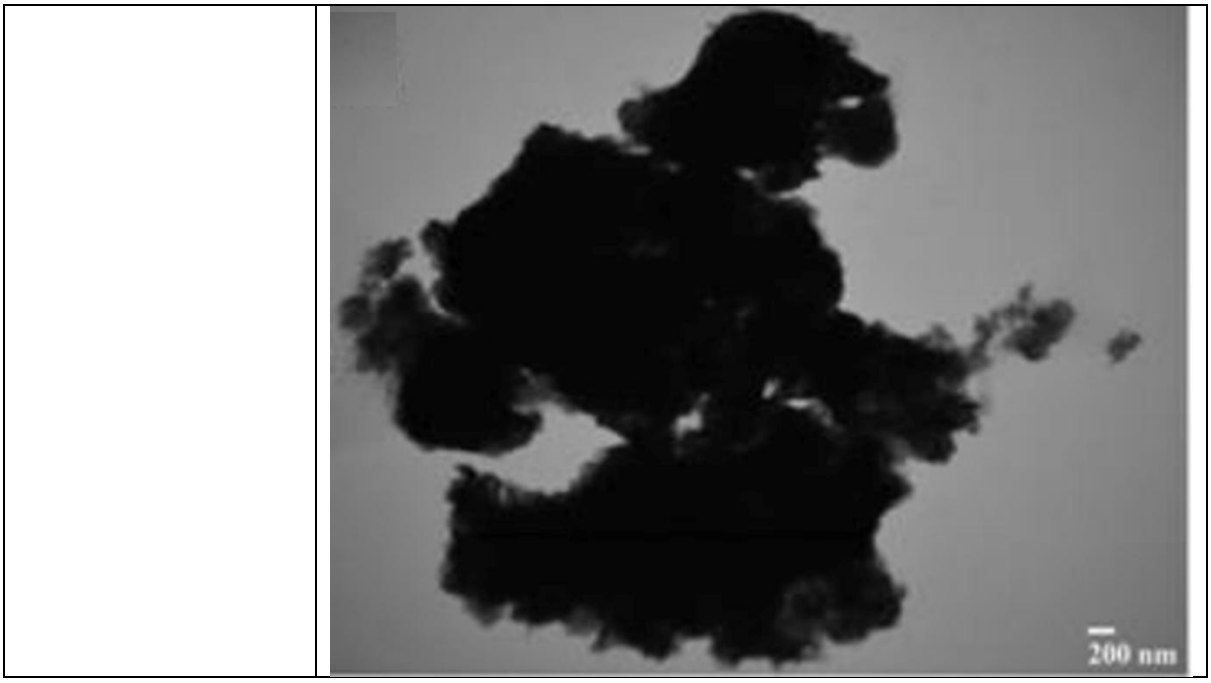

3.4.7 High-performance liquid chromatography (HPLC) of HS, Nanocomposite and biofertilizers

When HS, nanocomposite and biofertilizers are analysed using HPLC (High-Performance Liquid Chromatography), the results usually show how complicated and heterogeneous they are as shown in from **Fig. 8 to Fig. 12**. Humic compounds have broad, poorly defined peaks because they are mixes of a wide range of organic components. Their overlapping molecule sizes and polydisperse nature are the causes of this. Because humic substances contain conjugated double bonds, aromatic compounds, and other chromophores, they substantially absorb visible and ultraviolet light, especially in the 200–400 nm range. Due to differences in the components' charge density, hydrophobicity, or molecule sizes, the chromatogram may display a distribution of retention durations (López-Martínez et al., 2021; Ghani et al., 2021; Lu et al., 2022; Stefan-van Staden et al., 2024).

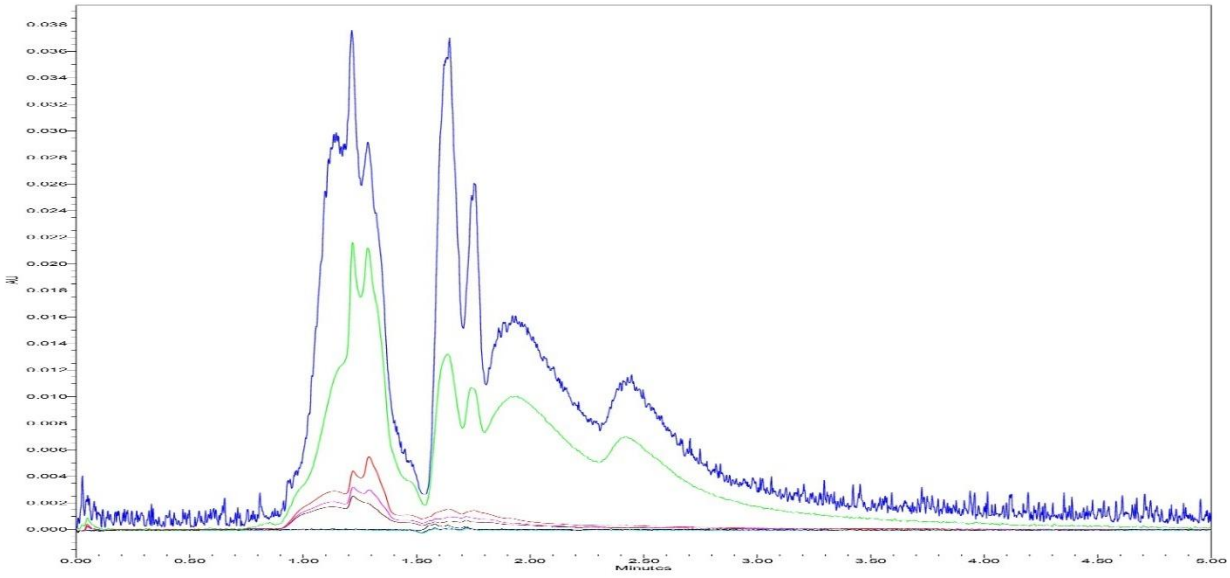

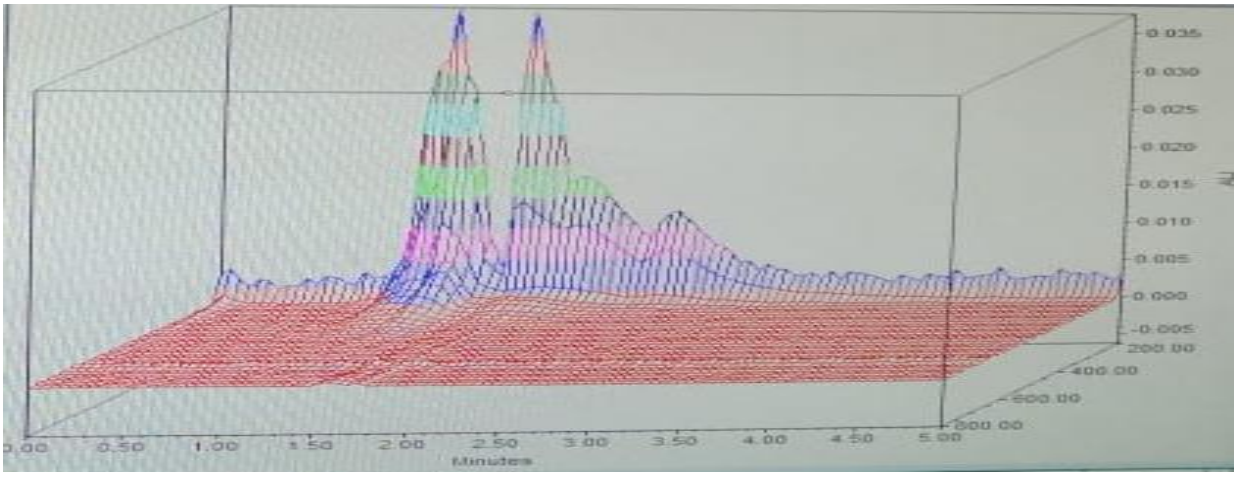

Fig. 8 (a) HPLC Analysis of Coal, FA, and HA

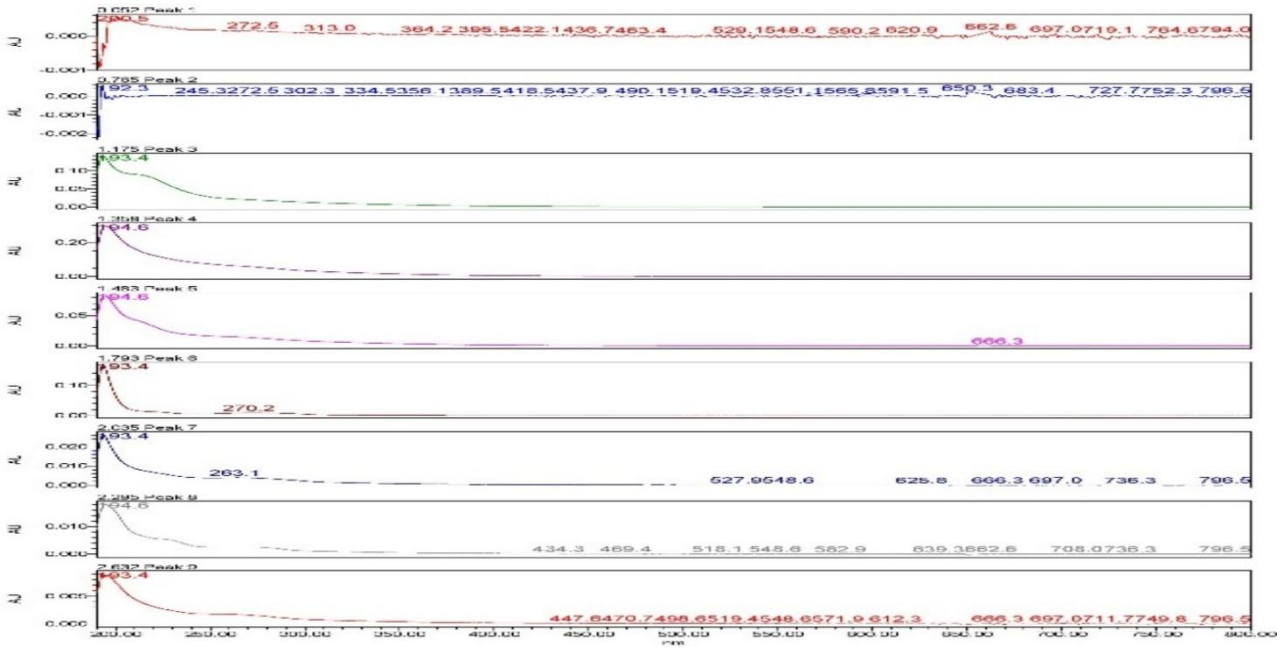

Fig. 8 (b) UV analysis of Coal, FA, and HA

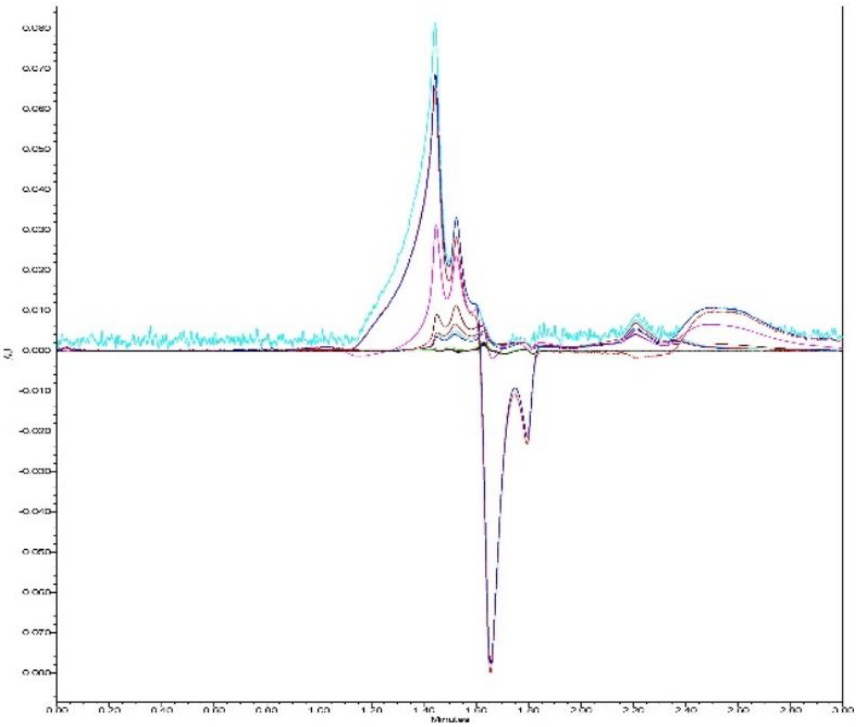

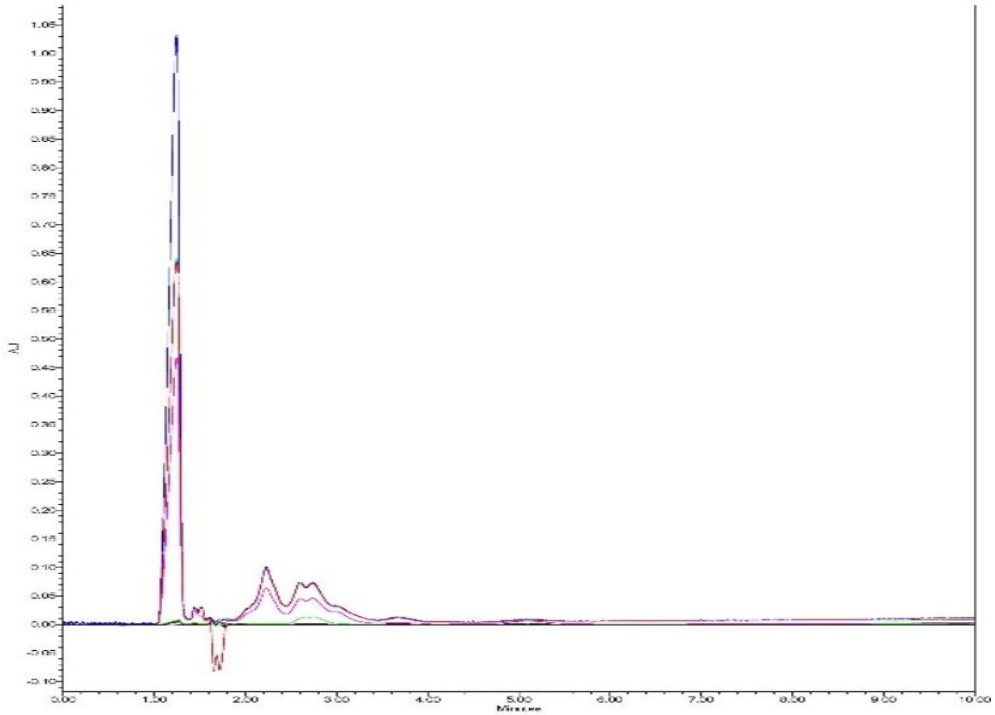

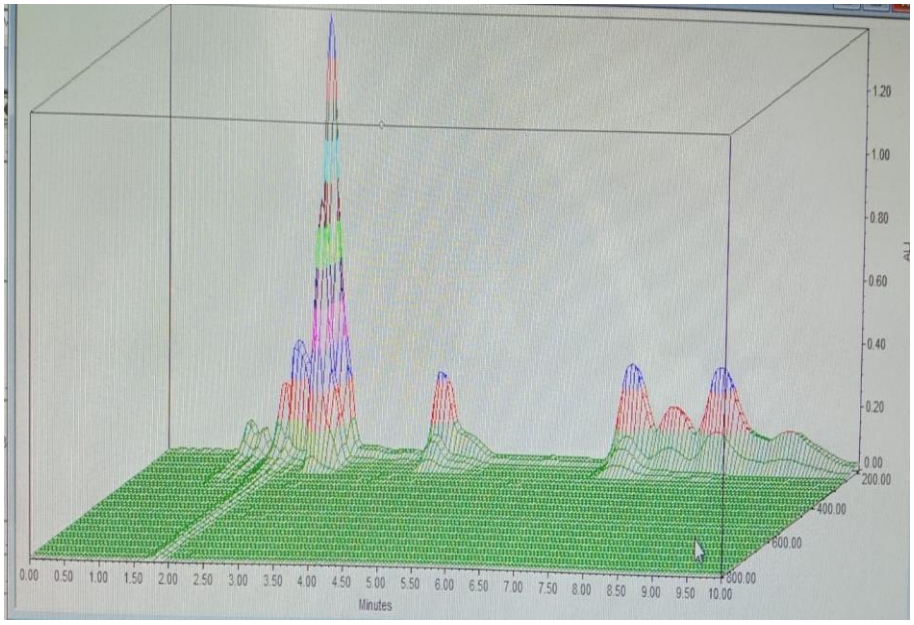

Fig. 9 (a) HPLC analysis of PGPB fortified FA complex

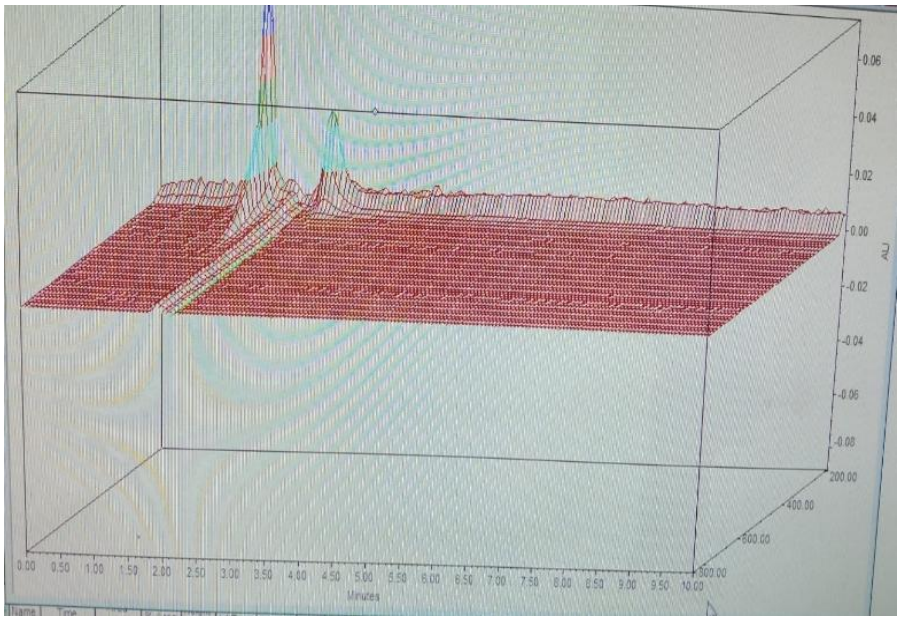

Fig. 9 (b) HPLC analysis of PGPB fortified HA complex

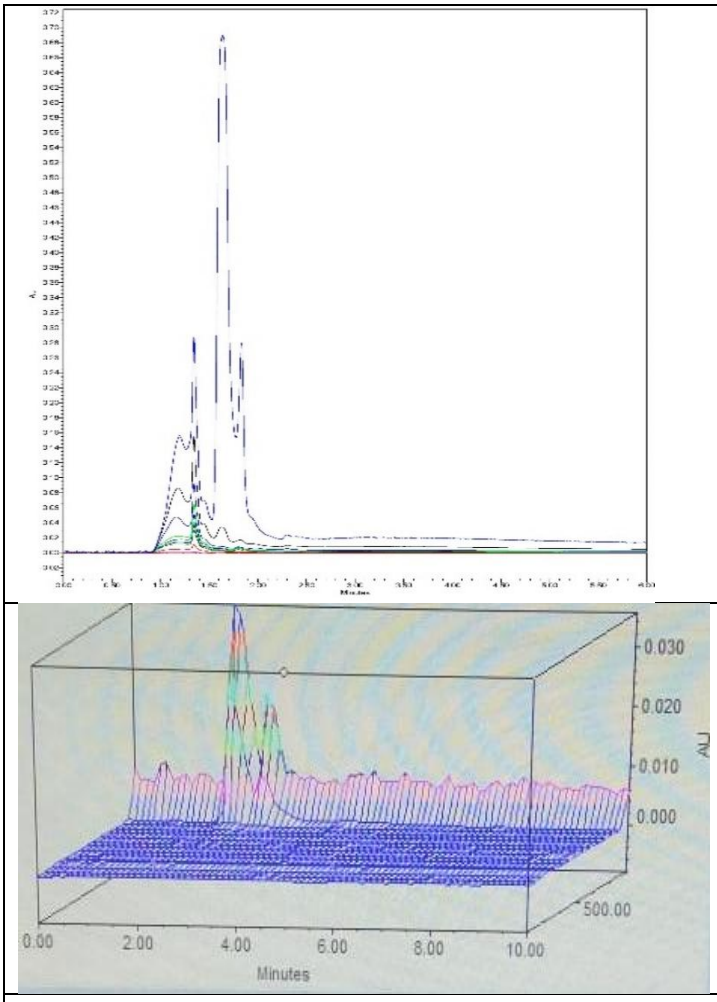

Fig. 10 (a) HPLC analysis of MgZn Ferrite composite fortified FA complex

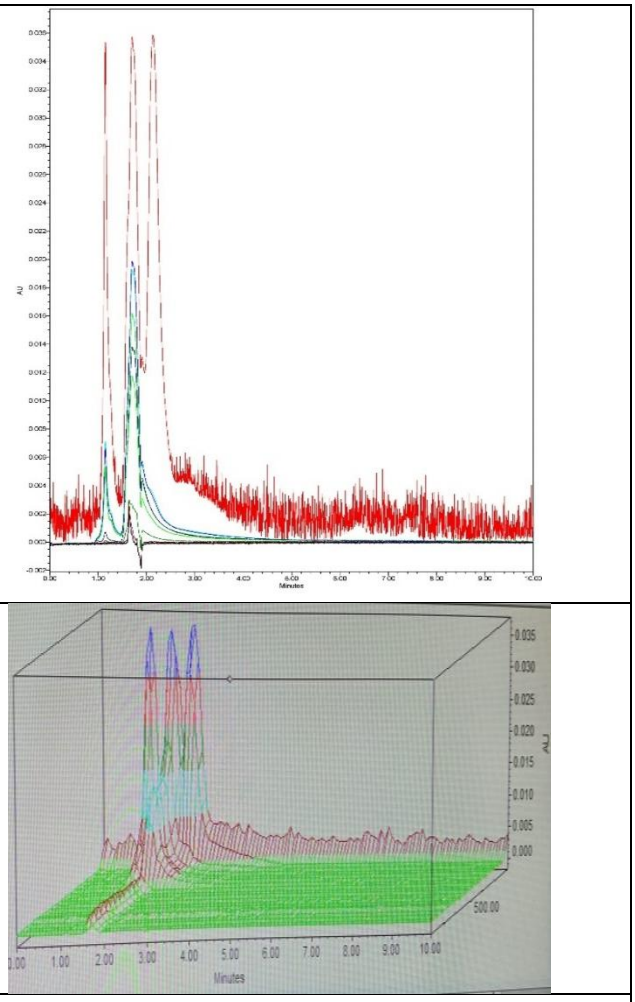

Fig. 10 (b) HPLC analysis of MgZn Ferrite composite fortified HA complex

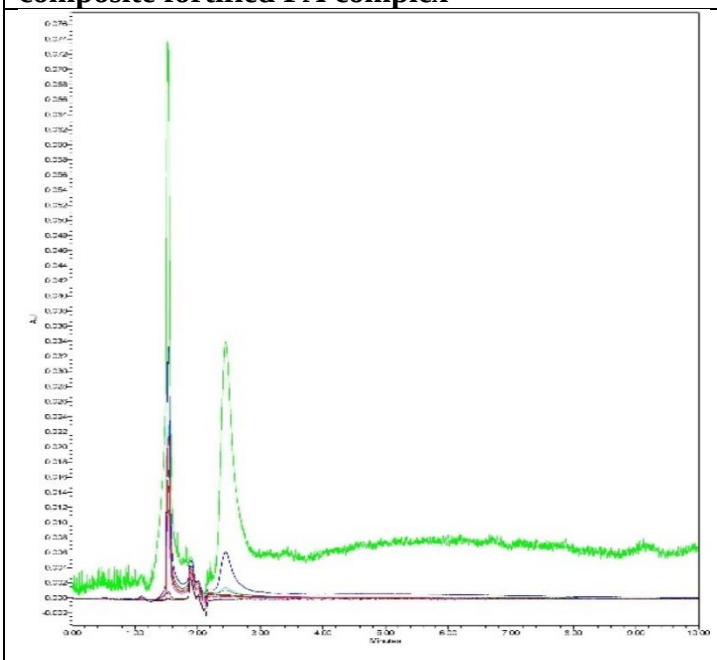

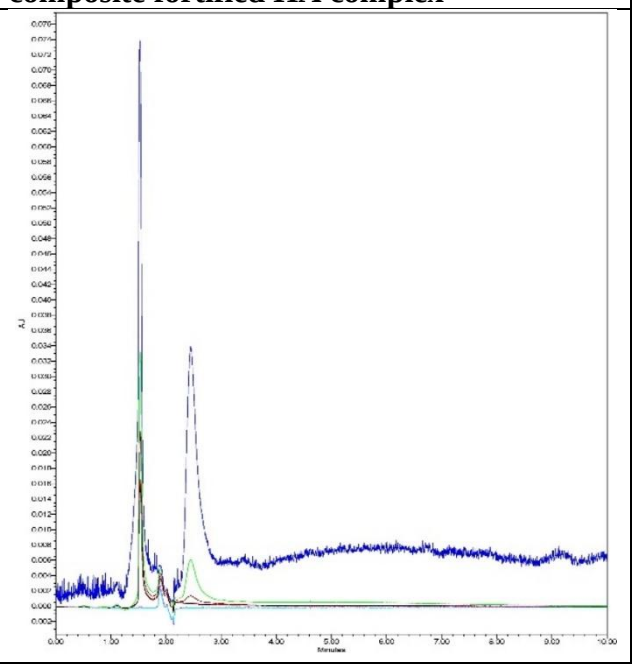

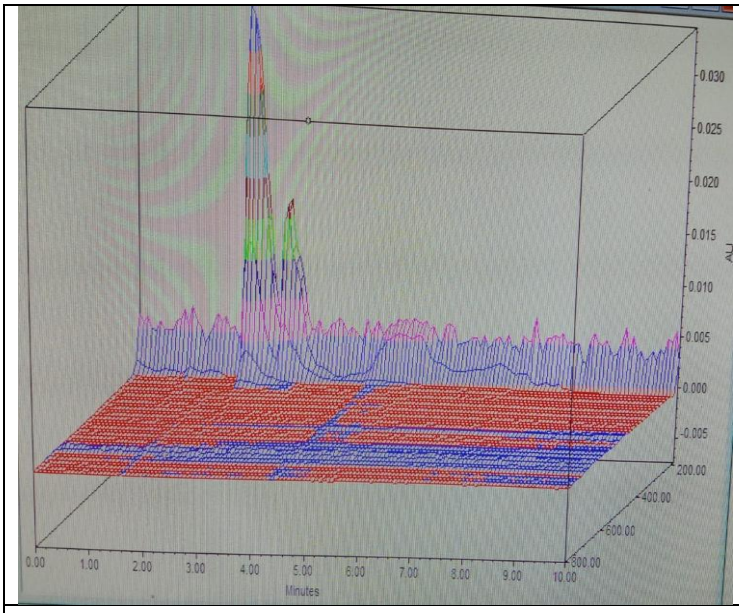

Fig. 11 (a) HPLC analysis of nutrients fortified FA

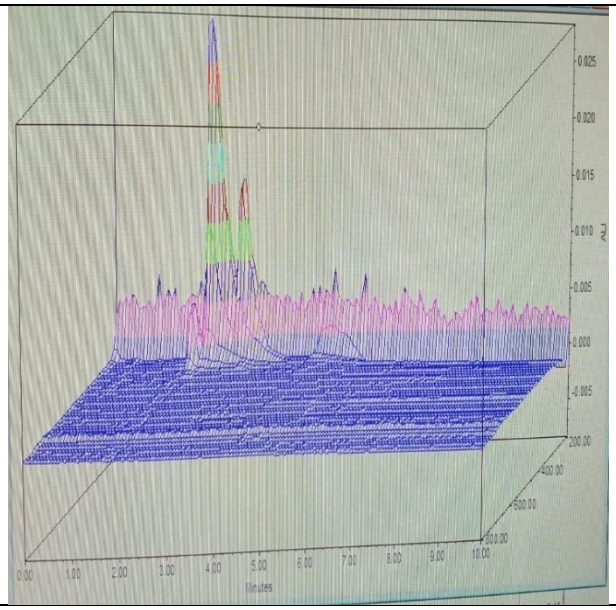

Fig. 11 (b) HPLC analysis of nutrients fortified HA

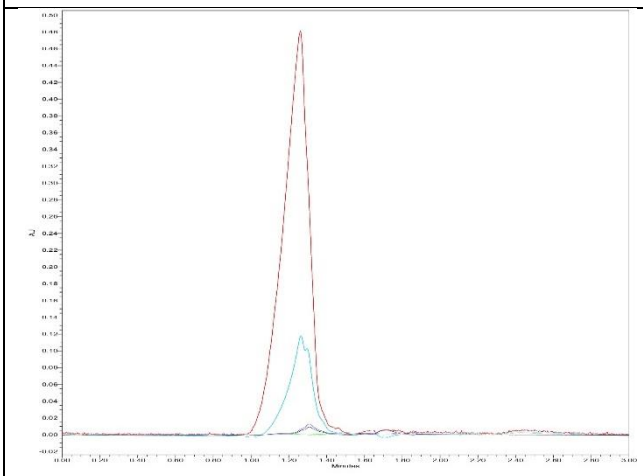

Fig. 12 (a) analysis of green synthesized MgZn Ferrite nanocomposite

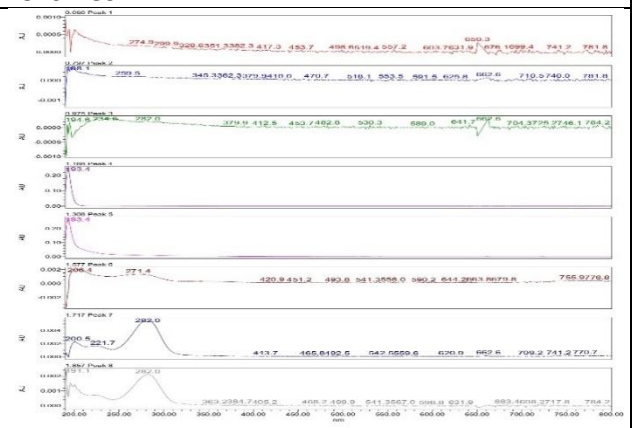

Fig. 12 (b) UV analysis of green synthesized MgZn Ferrite nanocomposite

CONCLUSION

All of Pakistan's provinces contain coal resources of 185 billion tones. In this paper we compared the synthesized bio, organic, and nano fertilizers which have a pH-buffering alkalinity, a cation exchange capacity, positive biological functions, and is widely used in agriculture. Using 0.1 M KOH, the coal samples collected from Punjab and Baluchistan, Pakistan, were examined for HS extraction. Following six hours of shaking, coal sample number 5 had the highest percentage yields of FA and HA (71.5% and 37.5%, respectively), while coal sample number 3 had the lowest yields of FA and HA (46.5% and 21.5%, respectively). The E4/E6 and E3/E5 ratios, which were calculated using UV-visible spectroscopy to evaluate the level of humification of HS samples, have the greatest values for sample no. 7's HA (1.99) and FA (222.52). Both gram-positive and gram-negative results were obtained from the PGPB isolates PSBW-R, KSBW-R, and AZOW-R. When the pH was raised from 8 to 10 and the temperature was raised to 40 and 50 ˚C, all isolates shown a favourable growth response and were able to metabolise various types of carbohydrates. Fourier transform infrared spectroscopy and HPLC were used to characterise the following: coal, HA, FA, macro and micronutrient fortified HS, PGPB fortified HS, and MgZn ferrite nano-composite fortified HS. XRD, DLS, SEM, and TEM were used to characterise the green synthesised nanocomposite. All fertilisers

have been shown to have intermolecular hydrogen bonds, aliphatic and aromatic hydrocarbons, and carboxylic acid, amino, and hydroxyl functional groups.

REFERENCES

1. Al-Hayani, A.S. and Sallume, M.O., 2023, August. Effect of Humic Acid and the Level of Nano and Conventional Nitrogen on the Available and Absorbed Nitrogen Element and the Potato Yield. In IOP Conference Series: Earth and Environmental Science (Vol. 1225, No. 1, p. 012002). IOP Publishing.
2. Al-Saif, A.M., Sas-Paszt, L., Awad, R.M. and Mosa, W.F., 2023. Apricot (Prunus armeniaca) Performance under Foliar Application of Humic Acid, Brassinosteroids, and Seaweed Extract. Horticulturae, 9(4), p.519.
3. Awais, M., Tariq, M., Ali, Q., Khan, A., Ali, A., Nasir, I.A. and Husnain, T., 2019. Isolation, characterization and association among phosphate solubilizing bacteria from sugarcane rhizosphere. *Cytology and Genetics*, *53*, pp.86-95.
4. Balasjin, N.M., Maki, J.S., Schläppi, M.R. and Marshall, C.W., 2022. Plant growth-promoting activity of bacteria isolated from Asian rice (Oryza sativa L.) depends on rice genotype. *Microbiology Spectrum*, *10*(4).
5. Chauhan, R. P. S., C. Gupta, and D. Prakash. 2012. Methodological advancements in green nanotechnology and their applications in biological synthesis of herbal nanoparticles. International Journal of Bioassays. 1(7): 6–10.
6. da Silva, M.S.R.D.A., dos Santos, B.D.M.S., da Silva, C.S.R.D.A., da Silva, C.S.R.D.A., Antunes, L.F.D.S., dos Santos, R.M., Santos, C.H.B. and Rigobelo, E.C., 2021. Humic substances in combination with plant growth-promoting bacteria as an alternative for sustainable agriculture. *Frontiers in Microbiology*, *12*, p.719653.
7. Dhayal, P., Age, A.B., Jadhao, S.D. and Magdum, A.A., 2023. Effect of enriched compost and humic acid on quality and nutrient status of soil after harvest of Safed Musli under inceptisols.
8. Din, M., Nelofer, R., Salman, M., Khan, F.H., Khan, A., Ahmad, M., Jalil, F., Din, J.U. and Khan, M., 2019. Production of nitrogen fixing Azotobacter (SR-4) and phosphorus solubilizing Aspergillus niger and their evaluation on Lagenaria siceraria and Abelmoschus esculentus. *Biotechnology Reports*, *22*, p.e00323.
9. Donahue, C. J and E. A. Rais. 2009. Proximate analysis of coal. Journal of Chemical Education. 86(2): 222-224.
10. Eshwar, M., M. Saliartha, K. B. Rekha and S. H. K. Sharma. 2017. Characterization of humic substances by functional groups and spectroscopic methods. International Journal of Current Microbiology and Applied Sciences. 6(10): 1768-1774
11. Ennan, Z., Zhu, Y., Hu, J. and Xu, T., 2022. Effects of humic acid organic fertilizer on soil environment in black soil for paddy field under water saving irrigation. Nature Environment and Pollution Technology, 21(3), pp.1243-1249.
12. Fatharani, R. and Rahayu, Y.S., 2018, November. Isolation and characterization of potassium-solubilizing bacteria from paddy rhizosphere (Oryza sativa L.). In *Journal of Physics: Conference Series* (Vol. 1108, No. 1, p. 012105). IOP Publishing.
13. Ghani, M.J., Akhtar, K., Khaliq, S., Akhtar, N. and Ghauri, M.A., 2021. Characterization of humic acids produced from fungal liquefaction of low-grade Thar coal. *Process Biochemistry*, *107*, pp.1-12.
14. Hansima, M.A.C.K., Jayaweera, A.T., Ketharani, J., Ritigala, T., Zheng, L., Samarajeewa, D.R., Nanayakkara, K.G.N., Herath, A.C., Makehelwala, M., Jinadasa, K.B.S.N. and Weragoda, S.K., 2022. Characterization of humic substances isolated from a tropical zone and their role in membrane fouling. *Journal of Environmental Chemical Engineering*, *10*(3), p.107456.
15. Ichwan, B., Eliyanti, E., Irianto, I. and Zulkarnain, Z., 2022. Combining humic acid with NPK fertilizer improved growth and yield of chili pepper in dry season. Advances in Horticultural Science, 36(4), pp.275-281

16. Jaeger, N. D., H. Demeyere, R. Finsy et al. 1991. Particle sizing by photon correlation spectroscopy. Part I. Monodisperse latices. Influence of scattering angle and concentration of dispersed material. Particle & Particle Systems Characterization. 8(1–4): 179–186.
17. Jarukas, L., Ivanauskas, L., Kasparaviciene, G., Baranauskaite, J., Marksa, M. and Bernatoniene, J., 2021. Determination of organic compounds, fulvic acid, humic acid, and humin in peat and sapropel alkaline extracts. *Molecules*, *26*(10), p.2995.
18. Li, S., Tan, J., Wang, Y., Li, P., Hu, D., Shi, Q., Yue, Y., Li, F. and Han, Y., 2022. Extraction optimization and quality evaluation of humic acids from lignite using the cell-free filtrate of Penicillium ortum MJ51. *RSC advances*, *12*(1), pp.528-539.
19. López-Martínez, V.G., Guerrero-Álvarez, J.A., Ronderos-Lara, J.G., Murillo-Tovar, M.A., Solá-Pérez, J.E., León-Rivera, I. and Saldarriaga-Noreña, H., 2021. Spectral characteristics related to chemical substructures and structures indicative of organic precursors from fulvic acids in sediments by NMR and HPLC-ESI-MS. *Molecules*, *26*(13), p.4051.
20. Lu, Z.H., Tian, Q., Zhou, D.D., Chen, M., Cao, Y.W., Zhuang, L.Y., Liu, X., Yang, Z.H. and Senosy, I.A., 2022. Magnetic MXene based metal organic frameworks composites: synthesis, characterization and application. *Journal of Environmental Chemical Engineering*, *10*(3), p.108037.
21. Malyushevskaya, A., Koszelnik, P., Yushchishina, A., Mitryasova, O., Mats, A. and Gruca-Rokosz, R., 2023. Eco-Friendly Principles on the Extraction of Humic Acids Intensification from Biosubstrates. Journal of Ecological Engineering, 24(2).
22. Mohite, B., 2013. Isolation and characterization of indole acetic acid (IAA) producing bacteria from rhizospheric soil and its effect on plant growth. *Journal of soil science and plant nutrition*, *13*(3), pp.638-649.
23. Nazarbek, U., Abdurazova, P. and Raiymbekov, Y., 2022. Extraction and Characterization of Humic Acid Based on Coal Mining Waste. *Chemical Engineering & Technology*, *45*(6).
24. Ndaba, B., Roopnarain, A., Haripriya, R.A.M.A. and Maaza, M., 2022. Biosynthesized metallic nanoparticles as fertilizers: An emerging precision agriculture strategy. *Journal of Integrative Agriculture*, *21*(5), pp.1225-1242.
25. Olivares, F.L., Aguiar, N.O., Rosa, R.C.C. and Canellas, L.P., 2015. Substrate biofortification in combination with foliar sprays of plant growth promoting bacteria and humic substances boosts production of organic tomatoes. *Scientia Horticulturae*, *183*, pp.100-108.
26. Panhwar, Q.A., Othman, R., Rahman, Z.A., Meon, S. and Ismail, M.R., 2012. Isolation and characterization of phosphate-solubilizing bacteria from aerobic rice. *African Journal of Biotechnology*, *11*(11), pp.2711-2719.
27. Rasouli, F., Nasiri, Y., Asadi, M., Hassanpouraghdam, M.B., Golestaneh, S. and Pirsarandib, Y., 2022. Fertilizer type and humic acid improve the growth responses, nutrient uptake, and essential oil content on Coriandrum sativum L. Scientific Reports, 12(1), p.7437.
28. Sable, P., Thabet, N., Yaseen, J. and Dharne, G., 2022. Effects on structural morphological and optical properties pure and cuo/zno nanocomposite. Trends in Sciences, 19(24), pp.3092-3092.
29. Saikia, B.K., Boruah, R.K. and Gogoi, P.K., 2007. FT-IR and XRD analysis of coal from Makum coalfield of Assam. *Journal of Earth System Science*, *116*, pp.575-579.
30. Salama, D.M., Abd El-Aziz, M.E., Osman, S.A., Abd Elwahed, M.S. and Shaaban, E.A., 2022. Foliar spraying of MnO2-NPs and its effect on vegetative growth, production, genomic stability, and chemical quality of the common dry bean. Arab Journal of Basic and Applied Sciences, 29(1), pp.26-39.
31. Sharif, A., Mustaqeem, M., Saleh, T.A., ur Rehman, A., Ahmad, M. and Warsi, M.F., 2022. Synthesis, structural and dielectric properties of Mg/Zn ferrites-PVA nanocomposites. *Materials Science and Engineering: B*, *280*, p.115689.
32. Stefan-van Staden, R.I., Dorneanu, A.E.S., Negut, C.C. and Stanciu, G., 2024. Fast Analysis of Humic Acid in Mud and Water Samples. *Journal of The Electrochemical Society*, *171*(11), p.117515.

33. Taha, T.A., Elrabaie, S. and Attia, M.T., 2018. Green synthesis, structural, magnetic, and dielectric characterization of NiZnFe 2 O 4/C nanocomposite. *Journal of Materials Science: Materials in Electronics*, *29*, pp.18493-18501.
34. Tahoun, A.M.A., El-Enin, M.M.A., Mancy, A.G., Sheta, M.H. and Shaaban, A., 2022. Integrative soil application of humic acid and foliar plant growth stimulants improves soil properties and wheat yield and quality in nutrient-poor sandy soil of a semiarid region. Journal of Soil Science and Plant Nutrition, 22(3), pp.2857-2871.
35. Tatarchuk, T., Myslin, M., Mironyuk, I., Bououdina, M., Pędziwiatr, A.T., Gargula, R., Bogacz, B.F. and Kurzydło, P., 2020. Synthesis, morphology, crystallite size and adsorption properties of nanostructured Mg–Zn ferrites with enhanced porous structure. *Journal of Alloys and Compounds*, *819*, p.152945.
36. Turan, M., Ekinci, M., Kul, R., Kocaman, A., Argin, S., Zhirkova, A.M., Perminova, I.V. and Yildirim, E., 2022. Foliar Applications of humic substances together with Fe/nano Fe to increase the iron content and growth parameters of spinach (Spinacia oleracea L.). Agronomy, 12(9), p.2044.
37. Venkateswarlu, S., B. N. Kumar, C.H. Prasad, P. Venkateswarlu and N.V.V. Jyothi. 2014. Bio-inspired green synthesis of Fe3O4 spherical magnetic nanoparticles using Syzygium cumini seed extract. Physica B: Condensed Matter. 449: 67-71.
38. Wang, X., Xie, H., Wang, P. and Yin, H., 2023. Nanoparticles in plants: Uptake, transport and physiological activity in leaf and root. *Materials*, *16*(8), p.3097.
39. Wu, D., Lu, Y., Ma, L., Cheng, J. and Wang, X., 2023. Preparation and Molecular Structural Characterization of Fulvic Acid Extracted from Different Types of Peat. *Molecules*, *28*(19), p.6780.
40. Zykova, M.V., Bratishko, K.A., Buyko, E.E., Azarkina, L.A., Ivanov, V.V., Mihalyov, D.A., Trofimova, E.S., Danilets, M.G., Ligacheva, A.A., Konstantinov, A.I. and Ufandeev, A.A., 2024. Coal-Derived Humic Substances: Insight into Chemical Structure Parameters and Biomedical Properties. *Molecules*, *29*(7), p.1530.